

## 季磷阳离子柱撑磷酸锆的热稳定性及抗菌活性

廖马花<sup>1</sup> 颜文艳<sup>1</sup> 蔡 祥<sup>1</sup> 张秀菊<sup>2</sup> 林志丹<sup>2</sup> 谭绍早<sup>\*,1</sup>

(<sup>1</sup>暨南大学化学系, 广州 510632)

(<sup>2</sup>暨南大学理工学院, 广州 510632)

**摘要:** 采用离子交换法将不同含量的十二烷基三丁基溴化磷(DDTB)插入层状磷酸锆得到一种耐高温且具有优良抗菌性能季磷阳离子柱撑磷酸锆(DDTB-ZrPs)。通过热重分析(TGA)、红外分析(FTIR)、X 射线衍射法(XRD)和透射电镜(TEM)对 DDTB-ZrPs 的结构进行了表征,并测定了 DDTB-ZrPs 的最低抑菌浓度。结果表明,季磷盐已经成功插入层状  $\alpha$ -磷酸锆的层间,DDTB-ZrPs 的层间距随着季磷盐含量的增加而增加。DDTB-ZrP-1(DDTB 含量为 5.61wt%)的热稳定性最好,有机物失重 5%时温度可达 320 °C,最大热分解率温度达 384 °C。DDTB-ZrP-6(DDTB 含量为 26.46wt%)显示出良好的长效抗菌活性,对大肠杆菌和金黄色葡萄球菌的最低抑菌浓度分别为 80 和 15 mg·L<sup>-1</sup>。进一步的研究表明,随着 DDTB 含量的增加,DDTB-ZrPs 的热稳定性降低而抗菌活性增强。

**关键词:**  $\alpha$ -磷酸锆; 十二烷基三丁基溴化磷; 热稳定性; 抗菌活性

中图分类号: O614.41<sup>2</sup>; O613.62

文献标识码: A

文章编号: 1001-4861(2011)05-0977-07

## Thermal Stability and Antibacterial Activity of Phosphonium Salts Pillared Layered $\alpha$ -Zirconium Phosphates

LIAO Ma-Hua<sup>1</sup> YAN Wen-Yan<sup>1</sup> CAI Xiang<sup>1</sup> ZHANG Xiu-Ju<sup>2</sup> LIN Zhi-Dan<sup>2</sup> TAN Shao-Zao<sup>\*,1</sup>

(<sup>1</sup>Department of Chemistry, Jinan University, Guangzhou 510632, China)

(<sup>2</sup>College of Science and Engineering, Jinan University, Guangzhou 510632, China)

**Abstract:** Dodecyl tributyl phosphonium bromide pillared layered  $\alpha$ -zirconium phosphate (DDTB-ZrPs) was prepared by introducing dodecyl tributyl phosphonium bromide (DDTB) into layered  $\alpha$ -zirconium phosphate (ZrP) through ion-exchange method, and the resulting DDTB-ZrPs were characterized by FTIR, XRD, TEM, and TGA/DTG techniques. Minimum inhibitory concentration (MIC) was used to evaluate antibacterial activity. The results show that the DDTB are intercalated into ZrP and the basal spacing of DDTB-ZrP is enlarged with the increase in phosphonium salt content. DDTB-ZrP-1 with 5.61wt% of DDTB, shows the highest temperature resistant, the 5% weight loss temperature could be up to 320 °C and the max decomposition rate temperature reaches to 384 °C. DDTB-ZrP-6 with 26.46wt% of DDTB displays the highest antibacterial activity for the MIC against *E. coli* and *S. aureus* of 80 and 15 mg·L<sup>-1</sup>, respectively. Further analyses indicate that along with the increase in the content of DDTB, the thermostability of DDTB-ZrPs decreases and the antibacterial activity improves.

**Key words:**  $\alpha$ -zirconium phosphate; dodecyl tributyl phosphonium bromide; thermal stability; antibacterial activity

In recent years, silver-based inorganic antibacterial materials have been studied as the preferred antimicrobials because of the advantages of

broad-spectrum, long-term resistant, excellent heat-resistant and high safety<sup>[1-3]</sup>. Nevertheless, applications of inorganic antibacterial agents are limited because of

收稿日期: 2010-09-14。收修改稿日期: 2010-12-22。

国家自然科学基金(No.20871058)资助项目。

\*通讯联系人。E-mail: tanshaozao@163.com

the high cost, easy discolor and poor mouldproof effects. So, researchers have turned their attention to the substitutes. Compare to inorganic antibacterial materials, organic antibacterial pillared clay minerals have attracted substantial attention both in fundamental research and industrial applications due to their superior antibacterial activity, good water resistance, high safety and the synergistic effect with other antimicrobial agents<sup>[4]</sup>. The main shortcomings of clay minerals are poor purity, large particle size with wide distribution, difficult for cleaning due to high viscosity. Therefore, it is necessary to seek for new intercalation materials without the shortcomings.

Zirconium bis-(monohydrogen orthophosphate) monohydrate ( $\text{Zr}(\text{HPO}_4)_2 \cdot \text{H}_2\text{O}$ ), also called layered  $\alpha$ -zirconium phosphate (ZrP), are drawing increasing attention because of its ability to serve as catalysts, solid electrolytes, and molecular sieves<sup>[5-7]</sup>. ZrP can also be used as host material to intercalate guest species, such as alkylamines, diamines and poly-amines, alkanols, glycols, urea and its derivatives, hydrazine, piperidine, dimethyl sulfoxide, dimethyl formamide, heterocyclic bases (imidazole, benzimidazole, alcohols and histamine), metal complexes, porphyrins, amino azobenzene<sup>[8-15]</sup>. Organic antibacterial material exchanged into ZrP may give novel antibacterial material with excellent antibacterial activity and high temperature resistance.

The main goal of this study is to develop a novel  $\alpha$ -ZrP based antibacterial material with high temperature resistance and good antibacterial activity. Here we report an antibacterial material obtained by intercalation of quaternary phosphonium cation into ZrP and the discussion on main factors affecting the temperature resistance and antibacterial activity.

## 1 Experimental

### 1.1 Materials

Zirconium oxychloride octahydrate ( $\text{ZrOCl}_2 \cdot 8\text{H}_2\text{O}$ , 98%) and phosphoric acid ( $\text{H}_3\text{PO}_4$ , volume fraction 85%) were obtained from Fisher Scientific. Dodecyl tributyl phosphonium bromide of C.P. grade was supplied by Qingte Chemical Industry Co., Ltd.

(Shanghai, China). *Escherichia coli* (*E. coli*) ATCC 25922 and *Staphylococci aureus* (*S. aureus*) ATCC 6538 were supplied by Guangdong Institute of Microbiology (Guangzhou, China). Mueller-Hinton broth and nutrient agar culture medium were from Huankai Microorganism Co, Ltd. (Guangzhou, China). All other chemicals were commercial available ones in reagent grade.

### 1.2 Preparation of DDTB pillared ZrP

ZrP was prepared by hydrothermal method. ZrP was used before intercalation with methylamine<sup>[16]</sup>. Dodecyl tributyl phosphonium bromide (DDTB) pillared ZrP was prepared by the following procedure:  $\alpha$ -ZrP was suspended in aqueous solutions of DDTBPBr at various DDTBP<sup>+</sup>/ZrP molar ratios (0.1:1, 0.25:1, 0.5:1, 1:1, 2:1 and 5:1) with constant stirring at 60 °C for 6 h producing DDTBP-intercalated ZrP materials with different loading levels. For example, the 1:1 DDTBP-exchanged ZrP material was prepared by suspending 0.1 mol of  $\alpha$ -ZrP in 500 mL of a 0.1 mol DDTBPBr aqueous solution. The mixture was filtered, and the solid was washed with distilled water until free from  $\text{Cl}^-$  ion as tested with 1%  $\text{AgNO}_3$  solution. After dried at 60 °C under vacuum for 2 d, This layered compound is white odorless and easy flow of powder, 300 mesh sieve rate of  $\geq 90\%$ . The resulting pillared layered compounds were designated as DDTB-ZrP-1, DDTB-ZrP-2, DDTB-ZrP-3, DDTB-ZrP-4, DDTB-ZrP-5 and DDTB-ZrP-6, respectively.

### 1.3 Characterization

Fourier transform infrared spectra (FTIR) were recorded with the Perkin-Elmer-Spectrum GX-Spectrophotometer using KBr pellet. X-ray diffraction (XRD) patterns of the DDTB-ZrPs were obtained using a Siemens D5000 powder diffractometer employing  $\text{Cu K}\alpha$  radiation ( $\lambda = 0.15418 \text{ nm}$ ) with a filtered flat LiF secondary beam monochromator. The X-ray tube was operated at 45 kV and 40 mA. All XRD patterns were collected with  $2\theta$  range of  $2.0^\circ \sim 40^\circ$  at a scanning rate of  $1^\circ \cdot \text{min}^{-1}$ . Thermogravimetric analysis (TGA) was conducted with a thermal analyzer (NETZSCH TG 209) under  $\text{N}_2$  flow, in a temperature range of  $40 \sim 900^\circ \text{C}$  and the scanning rate of  $10^\circ \text{C} \cdot \text{min}^{-1}$ . Transmission Electron

Microscopy (TEM) images were obtained with CM300 with an accelerating voltage of 200 kV.

#### 1.4 Antibacterial activity assay

The minimum inhibitory concentration (MIC) of DDTB-ZrPs against *E. coli* and *S. aureus* was measured by two-fold diluting method<sup>[17]</sup>. Briefly, DDTB-ZrPs were suspended into Mueller-Hinton broth medium to form homogeneous suspensions and then two-fold diluted into different concentrations. Each 1 mL of culture medium containing various concentrations of test sample was inoculated with 0.1 mL of 106 cfu · mL<sup>-1</sup> (Colony Forming Units · mL<sup>-1</sup>) bacterial suspension, cultured for 24 h at 37 °C under shaking, and then the growth of bacteria was observed. When no growth of bacteria was observed in the lowest concentration of test sample, the MIC of the sample was defined as this value of dilution, the test for every MIC of DDTB-ZrPs was repeated three times.

#### 1.5 Desorption test

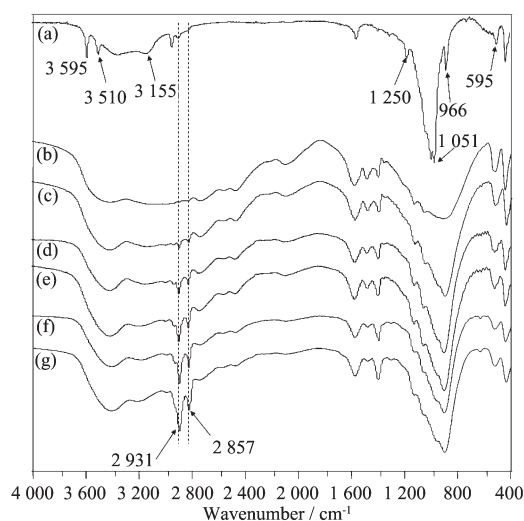
Desorption of phosphonium salts from DDTB-ZrPs was carried out by the process that 0.1 g sample was soaked in 20 mL deionized water in a polypropylene bottle at 40 °C on incubator shaker. As the experimental time was 6, 12, 24, 48, 60 and 72 h, the released quantity of DDTB from DDTB-ZrPs was measured by thermogravimetric analysis, and the MIC of soaked DDTB-ZrP against *E. coli* and *S. aureus* was also tested.

## 2 Results and discussion

### 2.1 Structure analysis

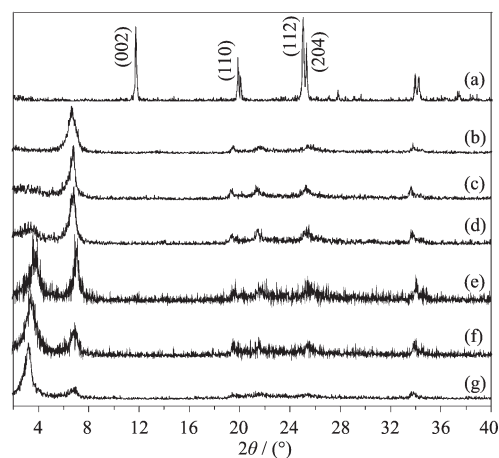
The FTIR spectra of ZrP and DDTB-ZrPs (Fig.1) show that the bands at 3 595, 3 510 and 3 155 cm<sup>-1</sup> are due to -OH stretching mode of P-OH of ZrP structure. The bands at 1 250 and 595 cm<sup>-1</sup> are caused by stretching vibration of in-plane deformation vibration of P-OH. The strong bands near 1 051 and 966 cm<sup>-1</sup> are probably caused by stretching vibration of P-O. The peaks at 2 931 and 2 857 cm<sup>-1</sup> are ascribed to the asymmetric and symmetric vibration of methylene groups (CH<sub>2</sub>)<sub>n</sub> of the aliphatic chain<sup>[18-19]</sup>.

Fig.2 shows the XRD patterns of ZrP and DDTB-ZrPs. The corresponding basal spacing ( $d_{002}$ ) is shown in Table 1, and results are summarized as follows: (1) XRD



(a) ZrP; (b) DDTB-ZrP-1; (c) DDTB-ZrP-2; (d) DDTB-ZrP-3; (e) DDTB-ZrP-4; (f) DDTB-ZrP-5; (g) DDTB-ZrP-6

Fig.1 FTIR spectra of a-ZrP and DDTB-ZrPs



(a) ZrP; (b) DDTB-ZrP-1; (c) DDTB-ZrP-2; (d) DDTB-ZrP-3; (e) DDTB-ZrP-4; (f) DDTB-ZrP-5; (g) DDTB-ZrP-6

Fig.2 XRD patterns of ZrP and DDTB-ZrPs

pattern of ZrP ( $d$ -spacings of 0.76, 0.44, 0.35 and 0.26 nm), all the above data agree with literature values<sup>[20-22]</sup> and displays structure similar to clays. The diffraction peak at  $2\theta=11.9^\circ$  is assigned to the basal spacing ( $d_{002}$ ) of 0.76 nm. The XRD patterns show the formation of a new phase with an expanded basal spacing of 1.28~2.58 nm which is much larger than that ( $d_{002}=0.76$  nm) of ZrP, and is attributed to the pillar of DDTB in the interlayer of ZrP. The basal spacing of DDTB-ZrPs is enlarged with the increasing of DDTB contents.

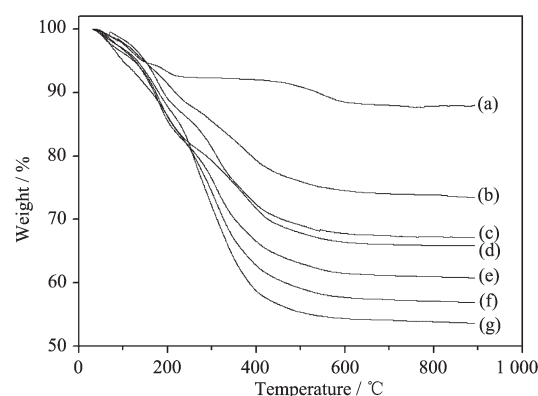
The thermogravimetric (TGA) curves of ZrP and DDTB-ZrPs are shown in Fig.3. According to the weight

**Table 1** Structure and property parameters for ZrP and DDTB-ZrPs

Samples	$d_{002}^b$ / nm	Phosphonium salt contents <sup>a</sup> / mass%	Temperature of 5% weight loss / °C	Temperatures of max decomposition rate / °C	$\zeta$ potentials / mV	Average particle size / nm
ZrP	0.76	—	—	—	-35.1	867
DDTB-ZrP <sub>0.1</sub>	1.28	5.61	320	384	-27.2	1 087
DDTB-ZrP <sub>0.25</sub>	1.28	7.25	300	377	-21.6	1 127
DDTB-ZrP <sub>0.5</sub>	1.32	13.60	261	320	-17.3	1 566
DDTB-ZrP <sub>1.0</sub>	2.42	22.34	260	313	-0.7	2 345
DDTB-ZrP <sub>2.0</sub>	2.52	25.09	258	310	0.4	2 578
DDTB-ZrP <sub>5.0</sub>	2.58	26.46	256	302	3.6	3 120

loss in the TG curves, the decomposition of ZrP clearly occurred in two general regions below 900 °C: (1) evaporation of free (absorbed) and interlayer water comprising the hydration spheres of the cations between 50~200 °C, (2) dehydroxylation of the ZrP lattice between 500~700 °C. In contrast, the TGA curves of DDTB-ZrPs may be conveniently divided into three regions<sup>[23]</sup>: (1) desorption of absorbed water and gases below 200 °C, (2) decomposition of the organic substances between 200~500 °C, (3) dehydroxylation of the ZrP lattice between 500~700 °C. So, the DDTB contents of DDTB-ZrPs could be determined in range (2) (200~500 °C), and the DDTB contents of DDTB-ZrPs are given in Table 1.

In this work, 5% weight loss temperature of DDTB is taken as an indicator of thermal stability of DDTB<sup>[24]</sup>, according to TGA curves, significant thermal degradation temperature of DDTB-ZrPs is given in Table 1. And the temperatures of max decomposition



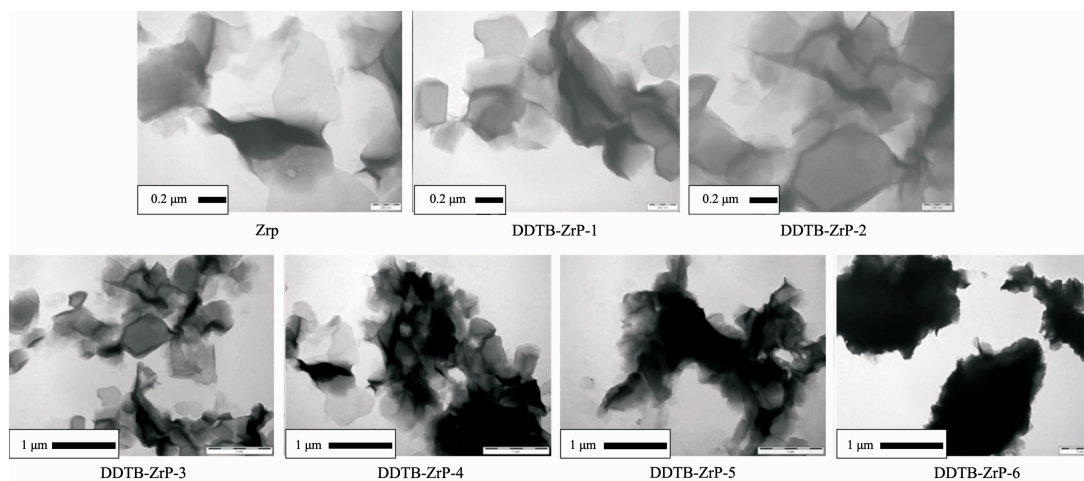
(a) ZrP; (b) DDTB-ZrP-1; (c) DDTB-ZrP-2; (d) DDTB-ZrP-3; (e) DDTB-ZrP-4; (f) DDTB-ZrP-5; (g) DDTB-ZrP-6

Fig.3 TGA curves of a-ZrP and DDTB-ZrPs

rate of DDTB-ZrPs are also given in Table 1.

So, the TG results indicate that with the increasing of the DDTB content, the 5% weight loss temperature and the max decomposition temperatures of the DDTB-ZrPs decrease.

TEM analysis (Fig.4) indicates that the crystal



(a) ZrP; (b) DDTB-ZrP-1; (c) DDTB-ZrP-2; (d) DDTB-ZrP-3; (e) DDTB-ZrP-4; (f) DDTB-ZrP-5; (g) DDTB-ZrP-6

Fig.4 TEM images of  $\alpha$ -ZrP and DDTB-ZrPs

layer of the DDTB-ZrPs was agglomerated than that of ZrP. With the increasing of the DDTB content, the crystal layer of the DDTB-ZrPs is agglomerated more. Zeta potential and average particle size of ZrP and DDTB-ZrPs (Table 1) show that: (1) with the increasing of the DDTB content, the  $\zeta$  potential of the DDTB-ZrPs is more positively charged, (2) with the increasing of the DDTB content, the particle size of the DDTB-ZrPs becomes larger.

## 2.2 Antibacterial activity

The antibacterial activity of ZrP and DDTB-ZrPs against *E. coli* and *S. aureus* is shown in Table 2. ZrP shows poor antibacterial activity (both of the MIC values are higher than  $20\,000\text{ mg}\cdot\text{L}^{-1}$ ). However, DDTB-ZrPs show relatively high antibacterial activity against *E. coli* and *S. aureus*, and the antibacterial activity enhances with the increasing of the phosphonium salt content.

Table 2 Antibacterial activity of DDTB-ZrPs

Samples	MIC / ( $\text{mg}\cdot\text{L}^{-1}$ )	
	<i>E. coli</i>	<i>S. aureus</i>
$\alpha$ -ZrP	>20000	>20000
DDTB-ZrP <sub>0.1</sub>	1000	400
DDTB-ZrP <sub>0.25</sub>	450	200
DDTB-ZrP <sub>0.5</sub>	200	50
DDTB-ZrP <sub>1.0</sub>	150	30
DDTB-ZrP <sub>2.0</sub>	100	20
DDTB-ZrP <sub>5.0</sub>	80	15

The IR and XRD results evidence the successful preparation of ZrP and formation of the pillared DDTB-ZrPs by DDTB intercalation between layers of ZrP. On the basis of the measured basal spacing and the length of the alkyl chains, various models have been proposed for the intercalated surfactants, including lateral-monolayer (LM), lateral-bilayer (LB), pseudo-trilayer (PT), paraffin-monolayer (PM) and paraffin-bilayer (PB)<sup>[25-26]</sup>. According to the data of van der Waals radius, covalent bond radius and bond angle, the steric configuration, size and shape of organic molecules or cations could be calculated<sup>[27]</sup>. In our study, the layer thickness of ZrP is 0.76 nm, with the increase of DDTB concentration, five typical basal spacings are obtained: (1)~1.28 nm, (2)~1.32 nm, (3)~2.42 nm, (4)~2.52 nm, (5)~2.58 nm, corresponding to the arrangement models of lateral-monolayer (DDTB-ZrP-1, DDTB-ZrP-2, DDTB-ZrP-3), lateral-monolayer add paraffin-monolayer (DDTB-ZrP-4, DDTB-ZrP-5, DDTB-ZrP-6), respectively. Simultaneously, the obviously transformation of the arrangement models of DDTB represent the products of the intermediate stage in the course of preparation of DDTB intercalated ZrP<sup>[26,28-29]</sup>.

The TG and DTG curves of the DDTB are represented in Fig.5. The 5% weight loss temperature of DDTB is 210 °C, and the max decomposition rate temperature is 248 °C.

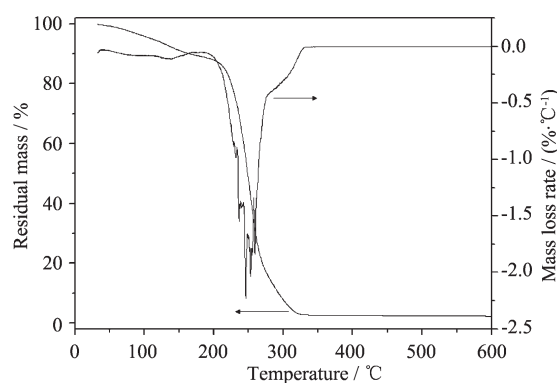


Fig.5 TG and DTG curves of the DDTB

On the other hand, the 5% weight loss temperatures of DDTB-ZrPs are all higher than 256 °C, and the max decomposition rate temperature are all higher than 302 °C. Which means DDTB pillared ZrP exhibits excellent thermal stability, can bear temperatures of nanocomposites processing during 200~300 °C. What is more, the ZrP with low-concentration DDTB exhibits better thermal stability, this may be that



with the increasing in the content of DDTB in ZrP, DDTB becomes more susceptible to heat.

TEM (Fig.4),  $\zeta$  potential and average particle size (Table 1) follows the same rule: with the increase of the DDTB content, the particle of the DDTB-ZrPs is agglomerated even more. This is due to negatively charged ZrP and positively charged DDTB. Following DDTB insertion into ZrP, the potential value of DDTB-ZrP gradually declines and the repelling force between particles gradually diminishes, thus more agglomeration.

DDTB-ZrPs show relatively high antibacterial activity against *E. coli* and *S. aureus*, and the antibacterial activity is enhanced with the increase in the phosphonium salt content. On the other hand, with the increase in the phosphonium salt content, the thermo tolerance of DDTB-ZrPs decreases. This means that the antibacterial activity and the thermo tolerance is a pair of incompatible system. And for industrial applications, one must find a balance point between the antibacterial activity and the thermo tolerance. In addition, DDTB-ZrPs exhibits lower activity against *E. coli* than against *S. aureus*. The structure of the cell wall

of *E. coli* is more complicated than that of the *S. aureus* because another layer outside of the peptidoglycan layer is called outer membrane, which is composed mainly of lipopolysaccharides and phospholipids. Outer membrane plays a significant role to protect bacteria cells from foreign compounds such as DDTB-ZrP. Thus, the lower sensitivity of DDTB-ZrPs towards *E. coli* is mainly due to the presence of the outer membrane<sup>[30]</sup>.

The stability of intercalated ZrP in water is evaluated, and the water resistance test of DDTB-ZrP-4 is given in table 3. During the first 48 h, DDTB is released quickly with the soaking time, and then released slowly. The released quantity of DDTB from DDTB-ZrP-4 is only 2.72% (mass fraction) until 72 h, testing for antibacterial activity of soaked DDTB-ZrP-4 (0.9%, mass fraction, 40 °C) is intended to study the effects of soaking time on the antibacterial activity of DDTB-ZrP, and the result is shown in Table 3. The MIC of DDTB-ZrP-4 against *E. coli* and *S. aureus* shows good antibacterial activity all the experimental time. And the MIC value is 300 mg·L<sup>-1</sup> and 180 mg·L<sup>-1</sup> MIC against *E. coli* and *S. aureus* until 72 h, respectively.

Table 3 Long- acting antibacterial activity of DDTB-ZrP<sub>1.0</sub>

Soaking time / h	Amount of released phosphonium salt / %	MIC / (mg·L <sup>-1</sup> )	
		<i>E. coli</i>	<i>S. aureus</i>
0	0	150	30
6	1.13	170	50
12	1.56	200	80
24	1.98	220	100
48	2.53	250	130
60	2.68	270	150
72	2.72	300	180

### 3 Conclusions

A high temperature resistant and predominant antibacterial material: DDTB pillared ZrP was developed, and the effects of microstructure on the thermal stability and antibacterial activity were studied. Comparing with DDTB, the thermostability of DDTB inserted ZrP is improved significantly, (2) with the increase in content of DDTB inserted into  $\alpha$ -ZrP, the

arrangement of DDTB changes from lateral-monolayer arrangement to paraffin-type monolayer arrangement, the potential value of DDTB-ZrPs gradually declines and the repelling force between particles gradually diminishes, the partial size of DDTB-ZrPs becomes larger and the antibacterial activity of DDTB-ZrPs becomes better, but the thermal stability of DDTB-ZrPs becomes worse, (3) the antibacterial activity and the thermo tolerance of DDTB-ZrPs is a pair of

incompatible system: along with the increase in the content of DDTB, the thermo tolerance of DDTB-ZrPs decreases, but the antibacterial activity improves.

**Acknowledgements:** This work was supported by the National Natural Science Foundation of P. R. China (No. 20676049, 20871058 and 20971028), the Foundation of Enterprise-University-Research Institute Cooperation from Guangdong Province and the Ministry of Education of China (Grant No. 2007B090400105 and 2008A010500005), and the Term Projects of Scientific Cultivation and Innovation Fund from Jinan University.

## References:

- [1] TAN Shao-Zao(谭绍早), DING Liu-Cai(丁刘才), LIU Ying-Liang(刘应亮), et al. *Chinese Chem. Lett. (Zhongguo Huaxue Kuaibao)*, **2007**, **18**(1):85-88
- [2] Zhang L Z, Yu J C, Yip H Y, et al. *Langmuir*, **2003**, **19**:10372-10380
- [3] Tan S Z, Zhang L L, Huang L H, et al. *J. Ceram. Soc. Jpn.*, **2007**, **115**:269-271
- [4] NI Jia-Za(倪嘉纘). *Rare-earth Bioinorganic Chemistry*(稀土生物无机化学). Beijing: Science Press, **2002**.
- [5] Clearfield A, Tindwa R M. *J. Inorg. Nucl. Chem.*, **1979**, **41**: 871-873
- [6] Karlsson M, Andersson C, Hjortkjaer J. *J. Mol. Catal. A-Chem.*, **2001**, **166**:337-339
- [7] Bermúdez R A, Colón Y, Tejada G A. *Langmuir*, **2005**, **21**:890-894
- [8] Bellezza F, Cipiciani A, Costantino U. *Langmuir*, **2002**, **18**: 8737-8742
- [9] Hoppe R, Alberti G, Costantino U, et al. *Langmuir*, **1997**, **13**: 7252-7257
- [10] Marta B V, Simon J K, Gary B H. *Chem. Mater.*, **2002**, **14**: 2656-2663
- [11] Kijima T, Machida S M. *Inorg. Chem.*, **1994**, **33**:2586-2591
- [12] Costantino U, Vivani R, Zima V. et al. *Langmuir*, **2002**, **18**: 1211-1217
- [13] Bellezza F, Cipiciani A, Costantino U. *Langmuir*, **2004**, **20**: 5019-5025
- [14] Vermeulen L A, Thompson M E. *Nature*, **1992**, **358**:656-658
- [15] Challa V, Kumar A C. *J. Am. Chem. Soc.*, **2000**, **122**:830-837
- [16] Sun L, Boo W J, Sue H J, et al. *Chem. Mater.*, **2007**, **19**:1749-1754
- [17] Kasuga N C, Sekino K, Koumo C, et al. *J. Inorg. Biochem.*, **2001**, **84**:55-65
- [18] Errera P, Burghardt R C, Phillips T D. *Vet. Microbiol.*, **2000**, **74**:259-272
- [19] Atel H A, Somani R S, Bajaj H C, et al. *Appl. Clay Sci.*, **2007**, **35**:194-200
- [20] Clearfield A, Duax W L, Medina A S, et al. *J. Phys. Chem.*, **1969**, **73**:3424-3430
- [21] Kijima T, Watanabe S, Machida M. *Inorg. Chem.*, **1994**, **33**: 2586-2591
- [22] Xu J, Li R K Y, Xu Y, et al. *Eur. Polym. J.*, **2005**, **41**:881-885
- [23] Xie W, Gao Z M, Pan W P, et al. *Chem. Mater.*, **2001**, **13**: 2927-2932
- [24] CAI Xiang(蔡祥), TAN Shao-Zao(谭绍早), LIAO Ma-Hua(廖马花), et al. *J. Cent. South Univ. Technol. (Zhongnan Daxue Xuebao)*, **2010**, **17**:485-491
- [25] Vaia R A, Teukolsky R K, Giannelis E P. *Chem. Mater.*, **1994**, **6**:1017-1022
- [26] ZHU Jian-Xi(朱建喜), HE Hong-Ping(何宏平), GOU Jiu-Gao(郭九皋), et al. *Chinese Sci. Bull. (Kexue Tongbao)*, **2003**, **48**: 368-372
- [27] ZHOU Gong-Du(周公度). *Inorganic Structural Chemistry*(无机结构化学). Beijing: Science Press, **1984**.
- [28] Tamura K, Nakazawa H. *Clay Miner.*, **1996**, **44**:501-505
- [29] He H P, Yang D, Yuan P, et al. *J. Colloid Interf. Sci.*, **2006**, **297**:235-243
- [30] Yoon K Y, Byeon J H, Park C W, et al. *J. Environ. Sci. Technol.*, **2008**, **42**:1251-1255